

Supplemental Material: Detailed Methodology

Whole-rock geochemical analyses

Thirty-six new analyses of felsic intrusive rocks are presented in this study. After weathered surfaces and cross-cutting veins were removed from the rock samples using a rock saw, the majority (34 of 36 total) were sent to the Ontario Geological Survey Geoscience Laboratories (Geolabs) for whole-rock litho-geochemical analysis. The rocks were pulverized using an agate mill. Major elements (Si, Ti, Al, Cr, Fe, Mn, Mg, Ca, Na, K, P; Table S1) and a set of trace elements (not reported here) were analysed by X-ray fluorescence (XRF). For XRF, samples are heated to 105 °C under nitrogen atmosphere and 1000°C under oxygen atmosphere and then fused with a borate flux. Samples were subsequently analysed using Malvern-Panalytical Axios Advanced WD-XRF spectrometers. Trace elements (including Ba, Be, Bi, Cd, Ce, Co, Cr, Cs, Cu, Dy, Er, Eu, Ga, Gd, Hf, Ho, In, La, Li, Lu, Mo, Nb, Nd, Ni, Pb, Pr, Rb, Sb, Sc, Sm, Sn, Sr, Ta, Tb, Th, Ti, Tl, Tm, U, V, W, Y, Yb, Zn, Zr; Table S1) were analysed by inductively coupled plasma mass spectrometry (ICP-MS). For ICP-MS, samples were first digested using a multi-acid solution in a closed vessel, before analysis using a Thermo Scientific iCAP-Q ICP-MS. The concentration of ferrous iron was measured using potentiometric titration with a permanganate solution standard. Water content was determined by heating samples to 105 °C to release free water and then 1000 °C for crystalline water; the concentration of water was subsequently measured by infrared absorption. Data quality was monitored by insertion of sample duplicates, internal reference materials and blanks.

One batch of samples (2 of 36 total) was sent to Activation Laboratories in Ontario for litho-geochemical analysis. Samples were crushed by a steel mill, fused using lithium metaborate/tetraborate, and digested in a weak nitric acid solution. Major elements (Si, Al, Fe, Mn, Mg, Ca, Na, K, Ti, P; Table S1) were analysed by ICP-optical emission spectrometry using a Varian Vista 735 ICP. Trace elements (Sc, Be, V, Cr, Ca, Ni, Cu, Zn, Ga, Ge, As, Rb, Sr, Y, Zr, Nb, Mo, Ag, In, Sn, Sb, Cs, Ba, La, Ce, Pr, Nd, Sm, Eu, Gd, Tb, Dy, Ho, Er, Tm, Yb, Lu, Hf, Ta, W, Tl, Pb, Bi, Th, U; Table S1) were measured by ICP-MS using a Perkin Elmer Sciex ELAN 6100 ICPMS. The concentration of ferrous iron was obtained by titration.

Mineral chemical analysis

Feldspar compositions (Table S2) were obtained by electron probe microanalysis (EPMA) at the Ontario Geological Survey Geolabs using a Cameca SX-100 Electron Probe Micro Analyser. Minerals were analysed using an accelerating voltage of 20 kV and beam current of 20 nA with an 8-micron rastered beam, and on-peak counting times were 10 s to 15 s. The data were acquired by wavelength-dispersive spectroscopy.

Concentrations of trace elements in plagioclase (Table S3) were measured by laser ablation ICP-MS at the Metal Isotope Geochemistry Laboratory at University of Waterloo. A 193 nm Analyte G2 laser ablation system coupled to an Agilent 8800 quadrupole ICP-MS were used for in situ analysis of plagioclase in standard size polished thin sections. A suite of elements (^{29}Si , ^{31}P , ^{39}K , ^{43}Ca , ^{47}Ti , ^{85}Rb , ^{88}Sr , ^{89}Y , ^{90}Zr , ^{93}Nb , ^{137}Ba , ^{139}La , ^{140}Ce , ^{141}Pr , ^{146}Nd , ^{147}Sm , ^{153}Eu , ^{157}Gd , ^{159}Tb , ^{163}Dy , ^{165}Ho , ^{166}Er , ^{169}Tm , ^{172}Yb , ^{175}Lu , ^{181}Ta , ^{208}Pb , ^{232}Th , ^{238}U) was measured during line scans with laser beam parameters of 110 μm spot diameter, 8 Hz, 4.50 J/cm², and of 3 $\mu\text{m/s}$ scan speed. Groups of three plagioclase line scans (~30 minutes) were bracketed by analysis of reference materials, including NIST-610 (primary standard), NIST-612, and BHVO-2G (secondary standards) at the same conditions with a reduced beam diameter of 65 μm . The data were processed using Iolite v4.4.5 (Paton et al., 2011) with internal standardization using ^{29}Si based on the average SiO_2 content of plagioclase in each sample from EPMA analyses. Segments of the line analyses were chosen for processing based on homogeneity and apparent lack of mineral

inclusions, however minor spatial variations in LREE concentrations were commonly present and could not be completely avoided. The limit of detection was calculated using the method of Howell et al. (2010). Measured concentrations of REE in NIST-612 and BHVO-2G were within 6% and 8% of accepted values respectively, except for overestimation of Lu in BHVO-2G by ~20%. Measured values from secondary reference materials are available in Table S3.

Calculation of the parental TTG composition for modeling

The modeled TTG composition (Table S4) was calculated by combining the median values for group 1 and 2 TTGs in proportions of 40% and 60% respectively to produce a theoretical parental melt composition with a neutral (1.00) Eu anomaly relative to chondrite-normalized REE values. Group 3 was not incorporated in the calculation because it constitutes a very minor volumetric component of the overall TTG population in the Wawa Gneiss Domain. Though multiple TTG parental melts may have existed in the region, we have elected to calculate a single, representative parental melt to simplify modeling and to allow the effect of fractionation and accumulation to be shown clearly. The approach of combining TTG group compositions was taken for three main reasons, 1) petrographic evidence supports the hypothesis that the groups represent cumulates and complementary melt-rich domains; 2) an insignificant Eu anomaly has classically been included in the geochemical definition of TTG (Moyen and Martin, 2012); and 3) the geochemical characteristics specific to the TTGs of the Wawa Gneiss Domain are incorporated into the parental melt. Other approaches for estimating an unmodified TTG composition, such as selecting a published melt composition obtained from basalt partial melting experiments (Rapp et al., 1991), require an assumed source composition that may not be appropriate for the Kapuskasing Uplift. For modeling, the concentration of H₂O and Fe₂O₃/FeO ratio of the parental melt composition were calculated from the measured values of the TTG samples, combining both the crystalline moisture and free moisture measurements for H₂O. We recognize the limitations of this approach, as these compositional parameters may be affected by post-crystallization processes; measures were taken in sample preparation to minimize inclusion of rock that underwent chemical changes after complete crystallization (see Whole-rock geochemical analyses).

Phase equilibrium modeling

Phase equilibrium modeling was done in the Na₂O–CaO–K₂O–FeO–MgO–Al₂O₃–SiO₂–H₂O–TiO₂–Fe₂O₃–Cr₂O₃ chemical system using the THERMOCALC software package, including THERMOCALC version 3.50 (Dec 2019), thermodynamic dataset version 6.33 (June 2017) of Holland and Powell (2011) and the igneous set of activity–composition models from Holland et al. (2018) (updated Dec 2019). Individual models are as follows: silicate melt (Holland et al., 2018); plagioclase (Holland and Powell, 2003); amphibole (Green et al., 2016); biotite (White et al., 2014); clinopyroxene (Holland et al., 2018); epidote (Holland and Powell, 2011); ilmenite (White et al., 2000). Quartz and water were modeled as pure phases.

A phase diagram (Fig. S1) was constructed from 0.4 GPa to 0.8 GPa and 400 °C to 1300 °C, with modeled phase assemblage boundaries calculated from the solidus (620 °C to 690 °C) to the liquidus (1150 °C to 1160 °C). The modal proportions of phases were calculated at 0.6 GPa from ~908 °C at 40 mol% plagioclase crystallization to ~1119 °C at 5 mol% plagioclase crystallization, with data collected from the model at 10 mol%, 15 mol%, 20 mol%, 25 mol%, 30 mol%, and 35 mol% plagioclase and at the calculated quartz-in and ilmenite-in boundaries. Further modeling below ~908 °C was not done, as amphibole is predicted to become stable beyond 40 mol% plagioclase crystallization (Fig. S1) and the interpreted cumulates (group 3) are predominantly composed of plagioclase and quartz, only rarely with

minor amphibole. The anorthite content of model plagioclase, as calculated by THERMOCALC, was also collected at each step.

Melt trace element modeling

Melt trace element modeling was done by a mass balance approach using the batch melting equation (Shaw, 1970):

$$\frac{C_L}{C_o} = \frac{1}{D(1 - F) + F}$$

where C_L is the concentration of an element in the melt, C_o is the concentration of the element in the system, D is the bulk distribution coefficient, and F is the melt fraction. The value for C_o for each element is the concentration calculated for the parental TTG composition (Table S4). For D , partition coefficients were calculated for plagioclase (Table S5) based on parameterizations developed by Bédard (2006). Partition coefficients for ilmenite are from Ewart and Griffin (1994) based on data from natural high-silica rhyolites. In our modeling, quartz was assumed to have no effect on the trace elements of interest.

Calculations using TTG compositions (natural samples and modeled melt)

The normative anorthite, albite, and orthoclase contents (Fig. 2) of the natural TTG samples were calculated using the GeoChemical Data toolkit (GCDkit) software Janoušek et al. (2006), the compositional fields of the granitoids are after Barker (1979). Trace element compositions of natural and modeled TTGs are normalized to the chondrite values of McDonough and Sun (1995) for spider diagrams and the calculation of the europium anomaly, which was done using the equation:

$$\frac{Eu}{Eu^*} = \frac{Eu_N}{\sqrt{Sm_N \times Gd_N}}$$

Supplemental text – Detailed methodology

Figure S1 – Phase diagram of the estimated parental TTG composition.

Figure S2 – Chondrite-normalized REE trends measured in plagioclase in TTGs. Limit of detection is shown where elemental abundance was too low to measure.

Table S1 – Whole-rock compositions of Wawa Gneiss Domain TTGs

Table S2 – Plagioclase major element analyses

Table S3 – Plagioclase trace element data

Table S4 – Calculated parental TTG composition

Table S5 – Partition coefficients calculated for model plagioclase and values from literature used for ilmenite

REFERENCES CITED

- Barker, F., 1979, Trondhjemite: Definition, environment and hypotheses of origin, *in* Developments in Petrology, Elsevier, v. 6, p. 1–12, doi:10.1016/B978-0-444-41765-7.50006-X.
- Bédard, J.H., 2006, Trace element partitioning in plagioclase feldspar: *Geochimica et Cosmochimica Acta*, v. 70, p. 3717–3742, doi:10.1016/j.gca.2006.05.003.
- Ewart, A., and Griffin, W.L., 1994, Application of proton-microprobe data to trace-element partitioning in volcanic rocks: *Chemical Geology*, v. 117, p. 251–284, doi:10.1016/0009-2541(94)90131-7.
- Green, E.C.R., White, R.W., Diener, J.F.A., Powell, R., Holland, T.J.B., and Palin, R.M., 2016, Activity–composition relations for the calculation of partial melting equilibria in metabasic rocks: *Journal of Metamorphic Geology*, v. 34, p. 845–869, doi:10.1111/jmg.12211.
- Holland, T., and Powell, R., 2003, Activity–composition relations for phases in petrological calculations: An asymmetric multicomponent formulation: *Contributions to Mineralogy and Petrology*, v. 145, p. 492–501, doi:10.1007/s00410-003-0464-z.
- Holland, T.J.B., and Powell, R., 2011, An improved and extended internally consistent thermodynamic dataset for phases of petrological interest, involving a new equation of state for solids: *Journal of Metamorphic Geology*, v. 29, p. 333–383, doi:10.1111/j.1525-1314.2010.00923.x.
- Holland, T.J.B., Green, E.C.R., and Powell, R., 2018, Melting of peridotites through to granites: A simple thermodynamic model in the system KNCFMASHTOCr: *Journal of Petrology*, v. 59, p. 881–900, doi:10.1093/petrology/egy048.
- Howell, D., Griffin, W.L., Pearson, N.J., Powell, W., Wieland, P., and O’Reilly, S.Y., 2013, Trace element partitioning in mixed-habit diamonds: *Chemical Geology*, v. 355, p. 134–143, doi:10.1016/j.chemgeo.2013.07.013.
- Janoušek, V., Farrow, C.M., and Erban, V., 2006, Interpretation of whole-rock geochemical data in igneous geochemistry: Introducing Geochemical Data Toolkit (GCDkit): *Journal of Petrology*, v. 47, p. 1255–1259, doi:10.1093/petrology/egl013.
- McDonough, W.F., and Sun, S.-s., 1995, The composition of the Earth: *Chemical Geology*, v. 120, p. 223–253, doi:10.1016/0009-2541(94)00140-4.

Moyen, J.-F., and Martin, H., 2012, Forty years of TTG research: *Lithos*, v. 148, p. 312–336, doi:10.1016/j.lithos.2012.06.010.

Paton, C., Hellstrom, J., Paul, B., Woodhead, J., and Hergt, J., 2011, Iolite: Freeware for the visualisation and processing of mass spectrometric data: *Journal of Analytical Atomic Spectrometry*, v. 26, 2508, doi:10.1039/c1ja10172b.

Rapp, R., Watson, E.B., and Miller, C.F., 1991, Partial melting of amphibolite/eclogite and the origin of Archean trondhjemites and tonalites: *Precambrian Research*, v. 51, p. 1–25, doi:10.1016/0301-9268(91)90092-O

Shaw, D.M., 1970, Trace element fractionation during anatexis: *Geochimica et Cosmochimica Acta*, v. 34, p. 237–243, doi:10.1016/0016-7037(70)90009-8.

White, R.W., Powell, R., Holland, T.J.B., and Worley, B.A., 2000, The effect of TiO₂ and Fe₂O₃ on metapelitic assemblages at greenschist and amphibolite facies conditions: Mineral equilibria calculations in the system K₂O–FeO–MgO–Al₂O₃–SiO₂–H₂O–TiO₂–Fe₂O₃: *Journal of Metamorphic Geology*, v. 18, p. 497–511, doi:10.1046/j.1525-1314.2000.00269.x.

White, R.W., Powell, R., Holland, T.J.B., Johnson, T.E., and Green, E.C.R., 2014, New mineral activity–composition relations for thermodynamic calculations in metapelitic systems: *Journal of Metamorphic Geology*, v. 32, p. 261–286, doi:10.1111/jmg.12071.

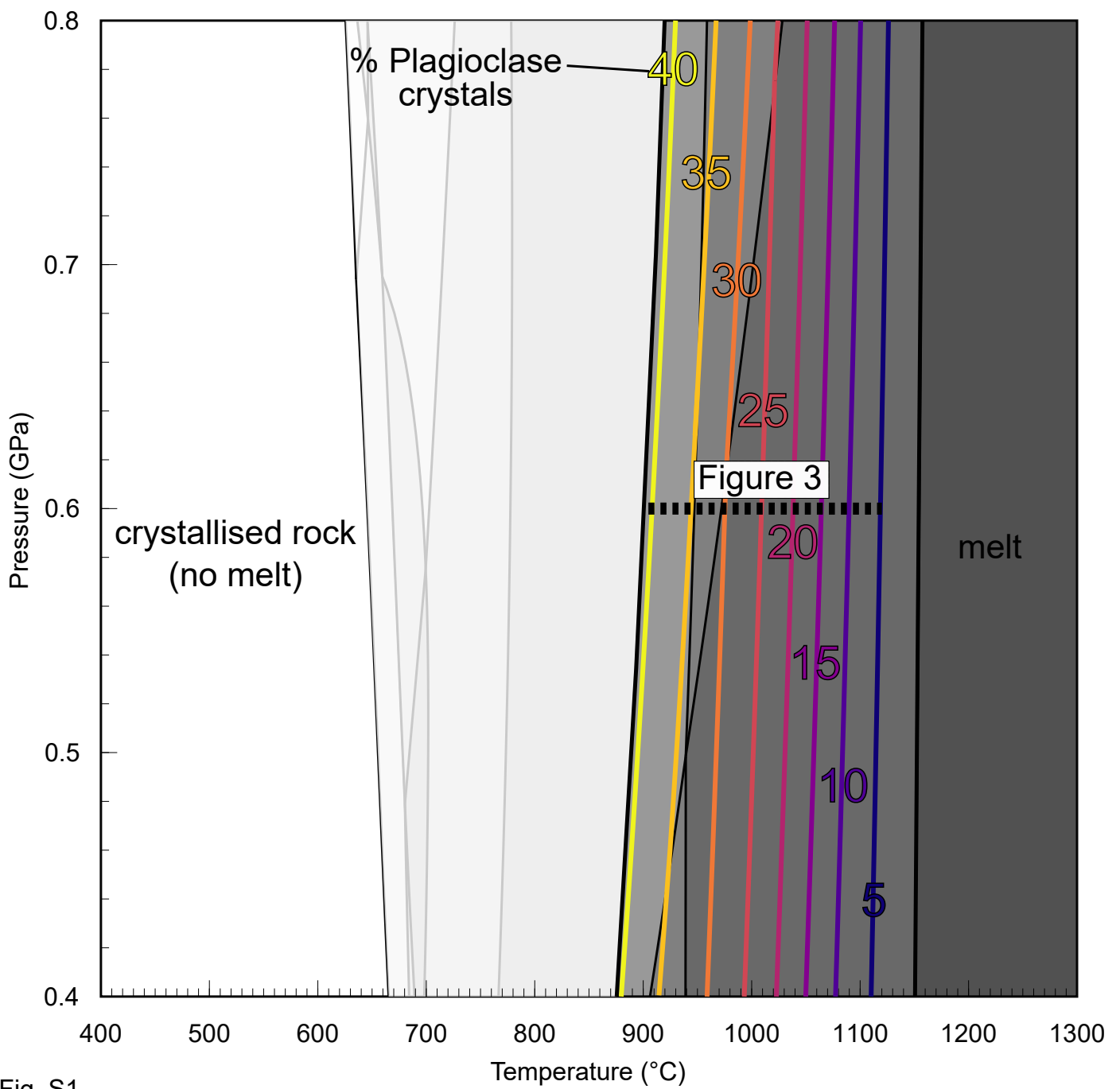
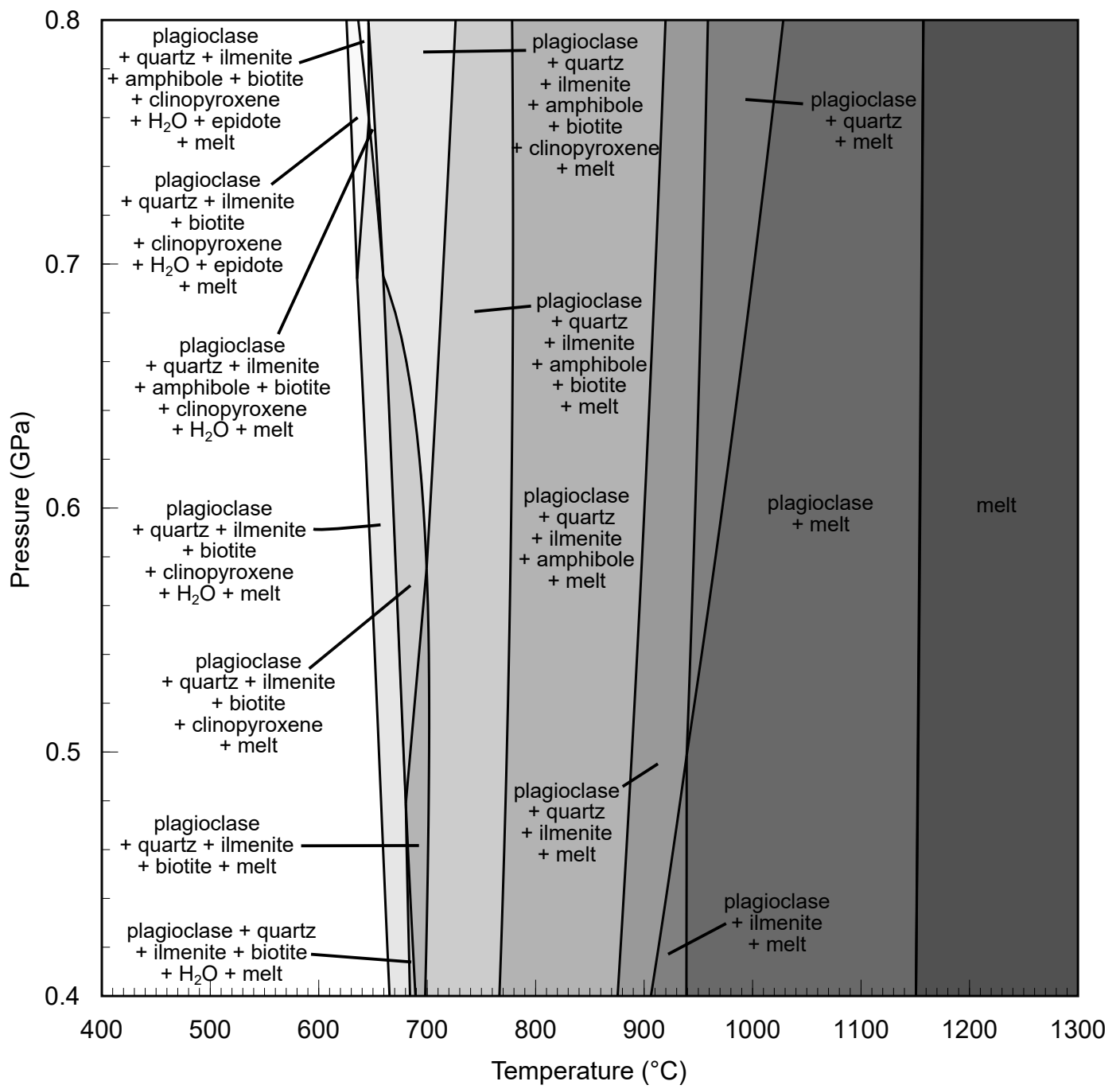


Fig. S1

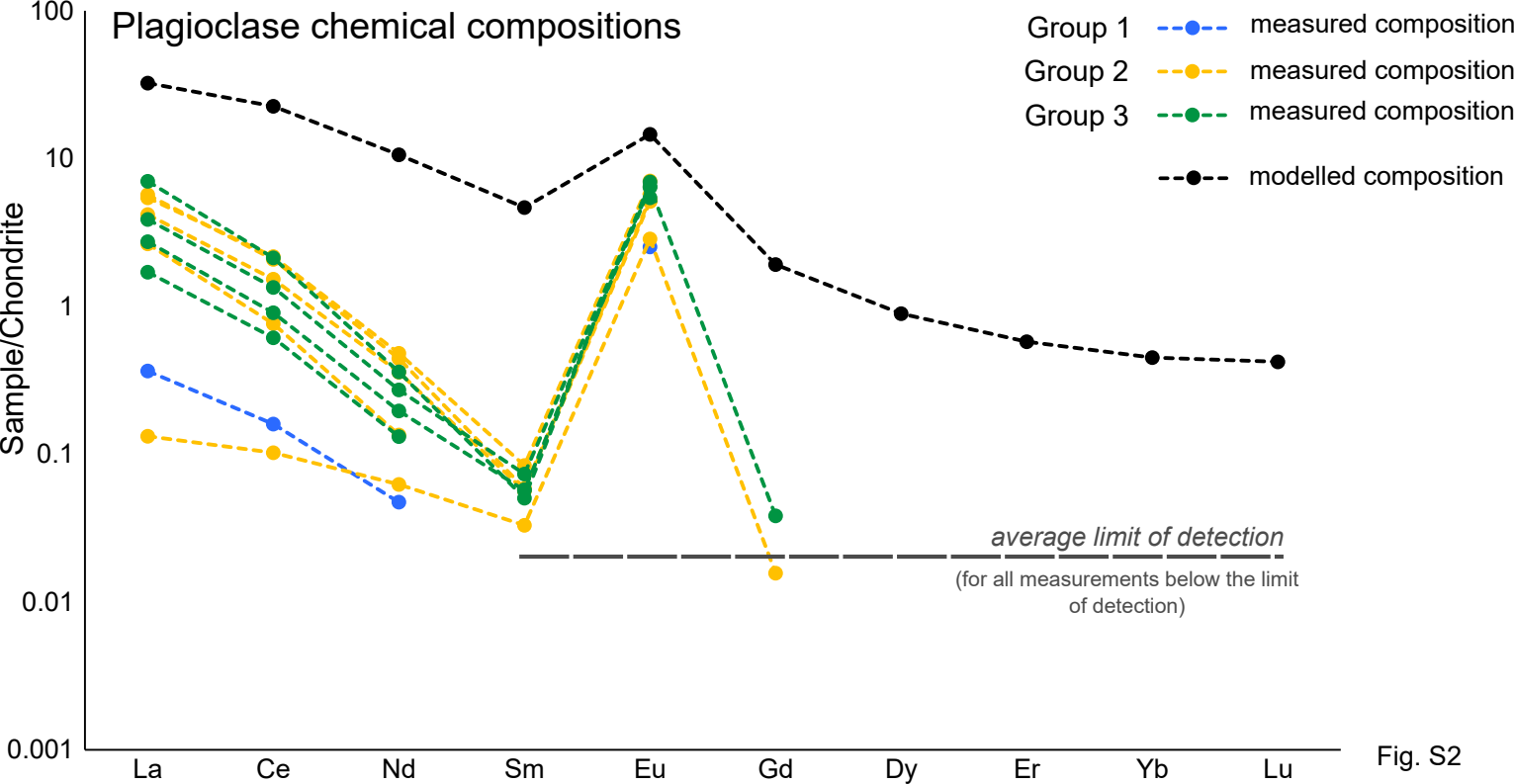


Fig. S2